AD-A108 195 MICHIGAN STATE UNIV EAST LANSING DEPT OF CHEMISTRY F/G 7/4
SOME COMPARISONS BETWEEN THE ENERGETICS OF ELECTROCHEMICAL AND --ETC(U)
NOV 81 M J WEAVER, J T HUPP N00014-79-C-0670
UNCLASSIFIED TR-6 NL

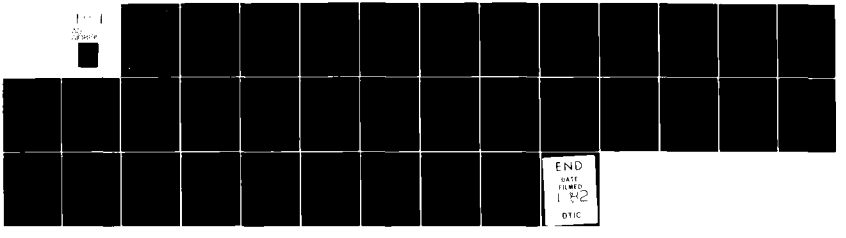

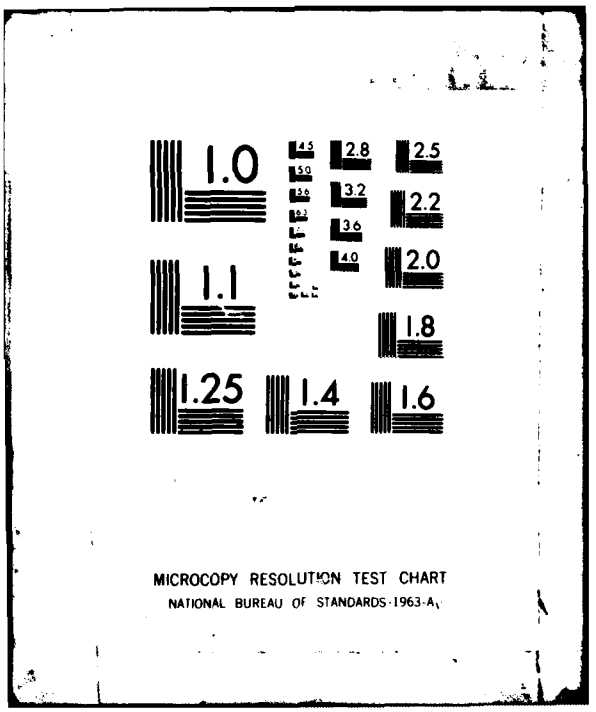
1.0
1.1
1.25
1.4
1.6
1.8
2.0
2.2
2.5
2.8
3.2
3.6
4.0
4.5
5.0
5.6
MICROCOPY RESOLUTION TEST CHART
NATIONAL BUREAU OF STANDARDS-1963-A

OFFICE OF NAVAL RESEARCH

Contract N00014-79-C-0670

TECHNICAL REPORT NO. 6

SOME COMPARISONS BETWEEN THE ENERGETICS OF ELECTROCHEMICAL AND HOMOGENEOUS ELECTRON-TRANSFER REACTIONS

by

Michael J. Weaver and Joseph T. Hupp

Prepared for Publication

in the

American Chemical Society Advances in Chemistry Series

Department of Chemistry

Michigan State University

East Lansing, MI 48824

November, 1981

SECURITY CLASSIFICATION OF THIS PAGE (When Data Entered)

REPORT DOCUMENTATION PAGE

READ INSTRUCTIONS BEFORE COMPLETING FORM

1. REPORT NUMBER: Technical Report No. 6	2. GOVT ACCESSION NO.: AD-A108195
3. RECIPIENT'S CATALOG NUMBER	
4. TITLE (and Subtitle): Some Comparisons Between the Energetics of Electrochemical and Homogeneous Electron-Transfer Reactions.	5. TYPE OF REPORT & PERIOD COVERED: Technical Report #6
	6. PERFORMING ORG. REPORT NUMBER
7. AUTHOR(s): Michael J. Weaver and Joseph T. Hupp	8. CONTRACT OR GRANT NUMBER(s): N00014-79-C-0670
9. PERFORMING ORGANIZATION NAME AND ADDRESS	10. PROGRAM ELEMENT, PROJECT, TASK AREA & WORK UNIT NUMBERS
11. CONTROLLING OFFICE NAME AND ADDRESS: Office of Naval Research, Department of the Navy, Arlington, VA 22217	12. REPORT DATE: November 23, 1981
	13. NUMBER OF PAGES
14. MONITORING AGENCY NAME & ADDRESS(if different from Controlling Office)	15. SECURITY CLASS. (of this report): Unclassified
	15a. DECLASSIFICATION/DOWNGRADING SCHEDULE

16. DISTRIBUTION STATEMENT (of this Report)

Approved for Public Release; distribution unlimited

17. DISTRIBUTION STATEMENT (of the abstract entered in Block 20, if different from Report)

18. SUPPLEMENTARY NOTES

19. KEY WORDS (Continue on reverse side if necessary and identify by block number)

Electrochemical Kinetics, Electron-Transfer Kinetics, Transition-Metal Aquo Complexes; Cobalt-Ammine Complexes

20. ABSTRACT (Continue on reverse side if necessary and identify by block number)

> Some conceptual relationships between the kinetics of corresponding electrochemical and homogeneous redox processes are discussed and applied to experimental data for suitable outer-sphere reactions in order to illustrate the utility of electrochemical kinetics for gaining some fundamental insights into the energetics of electron-transfer processes. It is pointed out that electrochemical kinetics and thermodynamics measurements as a function of temperature and electrode potential yield direct information on the shapes of the potential-energy surfaces and free energy barriers for *individual* redox couples. Comparisons

DD FORM 1 JAN 73 1473 EDITION OF 1 NOV 65 IS OBSOLETE S/N 0102-014-6601 |

Unclassified

SECURITY CLASSIFICATION OF THIS PAGE (When Data Entered)

between kinetics parameters for corresponding electrochemical and homogeneous exchange reactions show reasonable agreement with the predictions of the conventional ("weak overlap") model for several aquo redox couples, but exhibit substantial disagreement for couples containing amine and related ligands. These latter discrepancies may arise from the closer approach of the amine reactants to the electrode surface compared with the strongly solvated aquo complexes. A comparison is also made between the effects of varying the thermodynamic driving force upon the kinetics of related electrochemical and homogeneous reactions. It is shown that the apparent discrepancies seen between the predictions of the harmonic oscillator model and experimental data for some highly exoergic homogeneous reactions may be related to the anomalously small dependence of the rate constant upon overpotential observed for the electrooxidation of aquo complexes. This behavior seems most likely to be due to a marked asymmetry of the reactant and product free energy barriers for these half reactions.

Some Comparisons between the Energetics of Electrochemical and Homogeneous Electron-Transfer Reactions*.

Michael J. Weaver and Joseph T. Hupp

Department of Chemistry
Michigan State University
East Lansing, MI 48824

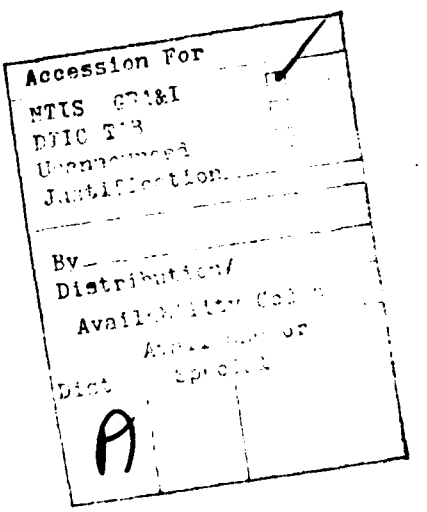

*Presented at the Conference on Inorganic Reaction Mechanisms, Wayne State University, June 1981.

Introduction

The kinetics of inorganic electrode reactions have long been the subject of experimental study. The advances in methodology, both in the precise treatment of mass transfer effects and the evolution of electrochemical relaxation techniques, have allowed the kinetics of a wide variety of electrode reactions to be studied. In addition, double-layer structural data are becoming available for a wide range of metal-electrolyte interfaces, which is enabling the kinetics of electrode reactions to be explored quantitatively in a variety of interfacial environments. However, electrode kinetics is noticeably underdeveloped in comparison with homogeneous redox kinetics, not only in terms of the availability of accurate kinetics data but also in the degree of molecular interpretation.

Nevertheless, simple electrochemical processes of the type

$$Ox + e^- \text{ (electrode, } \phi_m) \rightleftharpoons Red \qquad (1)$$

where both Ox and Red are solution species, form a valuable class of reactions with which to study some fundamental features of electron transfer in condensed media. Thus such processes involve the activation of only a single redox center, and the free energy driving force can be continuously varied at a given temperature simply by altering the metal-solution potential difference ϕ_m by means of an external potential source. In addition, electrode surfaces may exert only a weak electrostatic influence upon the energy state of the reacting species, so that in some cases they could provide a good approximation to the "outer-sphere, weak overlap" limit described by conventional electron-transfer theory. Electrochemical kinetics therefore provides a unique opportunity to examine *separately* the reaction energetics of individual redox couples ("half-reactions") which can only be studied in tandem in homogeneous solution. In this paper, some relationships between the kinetics of heterogeneous and homogeneous redox processes are explored in order to illustrate the utility of electrochemical kinetics and thermodynamics for gaining fundamental insights into the energetics of outer-sphere electron transfer.

Electrochemical Rate Formulations

Similarly to homogeneous electron-transfer processes, one can consider the observed electrochemical rate constant k_{ob} to be related to the electrochemical free energy of reorganization for the *elementary* electron-transfer step ΔG^* by

$$k_{ob} = A \exp(-w_p)\exp(-\Delta G^*/RT) \qquad (2)$$

where A is a frequency factor, and w_p is the work required to transport the reactant from the bulk solution to a site sufficiently close to the electrode surface ("precursor" or "pre-electrode" state) so that thermal reorganization of the appropriate nuclear coordinates can result in electron transfer. Also, for one-electron electroreduction reactions [Eqn. (1)] ΔG^* can usefully be separated into "intrinsic" and "thermodynamic" contributions according to[1-3]

$$\Delta G^* = \Delta G^*_{ie} + \alpha[F(E - E^\circ) + w_s - w_p)] \qquad (3)$$

where E is the electrode potential at which k_{ob} is measured, E° is the standard (or formal) potential for the redox couple concerned, w_s is the work required to transport the product from the bulk solution to the "successor" state which is formed immediately following electron transfer, α is the (work-corrected) electrochemical transfer coefficient, and ΔG^*_{ie} is the "intrinsic" free energy of activation for electrochemical exchange.[3] This last term equals ΔG^* for the particular case when the precursor and successor states have equal energies, i.e. when the free energy driving force for the elementary reaction $[F(E - E^\circ) + w_s - w_p]$ equals zero. The electrochemical transfer coefficient α reflects the extent to which ΔG^* is altered when this driving force is nonzero; α therefore provides valuable information on the symmetry properties of the elementary electron-transfer barrier.[4]

It is conventional (and useful) to define a "work-corrected" rate constant k_{corr} that is related to k_{ob} at a given electrode potential by

$$k_{corr} = k_{ob} \exp\{[w_p + \alpha(w_s - w_p)]/RT\} \quad (4)$$

This represents the value of k_{ob} that (hypothetically) would be obtained at the same electrode potential if the work terms w_p and w_s both equalled zero. For outer-sphere reactions, the work terms can be calculated approximately from a knowledge of the average potential on the reaction plane ϕ_{rp}, since $w_p = ZF\phi_{rp}$ and $w_s = (Z - 1)F\phi_{rp}$, where Z is the reactant's charge number. Eqn. (4) can then be written as

$$k_{corr} = k_{ob} \exp\{[(Z - \alpha)F\phi_{rp}]/RT\} \quad (5)$$

Usually ϕ_{rp} is identified with the average potential across the diffuse layer ϕ_d^{GC} as calculated from Gouy-Chapman theory using the diffuse-layer charge density obtained from thermodynamic data. In view of the usefulness of k_{corr}, it is also convenient to define a "work-corrected" free energy of activation ΔG_e^* at a given electrode potential, which is related to k_{corr} by [cf. Eqn. (2)]:

$$k_{corr} = A \exp(-\Delta G_e^*/RT) \quad (6)$$

so that Eqn. (3) can be written simply as

$$\Delta G_e^* = \Delta G_{ie}^* + \alpha F(E - E^\circ) \quad (7)$$

Therefore the value of k_{corr} measured at E°, i.e. the "standard" rate constant k_{corr}^s, is directly related to the intrinsic barrier ΔG_{ie}^*.

In addition, temperature derivatives of k_{corr} can be measured which allows the enthalpic and entropic components of ΔG_e^* to be obtained. Here an apparent difficulty arises in that a multitude of different Arrhenius plots may be obtained for an electrochemical reaction at a given electrode potential (inevitably measured with respect to some reference electrode), depending upon the manner in which the electrical variable is controlled as the temperature

is varied. However, two types of electrochemical activation parameters provide particularly useful information.[5-8] The first type, which have been labelled "real" activation parameters[5,6] (ΔH_r^*, ΔS_r^*), are extracted from an Arrhenius plot of k_{corr}^s as a function of temperature. The significance of these quantities is analogous to that for the activation parameters for homogeneous self-exchange reactions. Thus ΔH_r^* equals the activation enthalpy for conditions where the enthalpic driving force ΔH_{rc}° for the electrochemical reaction (1) equals zero. Similarly, ΔS_r^* equals the activation entropy for the (albeit hypothetical) circumstance where the entropic driving force ΔS_{rc}° (the "reaction entropy"[9]) is zero.[6] The quantities ΔH_r^* and ΔS_r^* are therefore equal to the "intrinsic" enthalpic and entropic barriers, ΔH_{ie}^* and ΔS_{ie}^*, respectively, which together constitute the intrinsic free energy barrier ΔG_{ie}^*. However, although the activation free energy ΔG_e^* determined at E° will equal ΔG_{ie}^* [Eqn. (7)], the enthalpic and entropic barriers at E°, ΔH_e^* and ΔS_e^*, will differ from ΔH_{ie}^* and ΔS_{ie}^*. This is because at E°, generally $\Delta S_{rc}^\circ \neq 0$,[9] and since $\Delta H_{rc}^\circ = T\Delta S_{rc}^\circ$, then $\Delta H_{rc}^\circ \neq 0$.

Reasonable estimates of ΔH_e^* and ΔS_e^* at a given electrode potential can be obtained from an Arrhenius plot measured at the required electrode potential held constant *at all temperatures* using a "nonisothermal cell" arrangement with the reference electrode compartment maintained at a fixed temperature.[8] These quantities, which have been termed "ideal" activation parameters ΔH_i^* and ΔS_i^*, can be identified with $\Delta \bar{H}_e^*$ and $\Delta \bar{S}_e^*$ since the use of such a nonisothermal cell maintains the Galvani metal-solution potential difference ϕ_m, and hence the energy of the reacting electron, essentially constant as the temperature is varied.[8,9]

Similarly, the reaction entropy ΔS_{rc}° for a given redox couple can be determined from the temperature derivative of the standard potential E_{ni}°

measured using a nonisothermal cell, i.e. $\Delta S^\circ_{rc} = F(dE^\circ_{ni}/dT)$, since (dE°_{ni}/dT) should approximately equal the desired temperature dependence of the standard Galvani potential $(d\phi^\circ_m/dT)$.[9] The reaction entropy provides a useful measure of the changes in the extent of solvent polarization for a single redox couple brought about by electron transfer.[9] Since $\Delta G^\circ_{rc} = F(E - E^\circ)$, the corresponding enthalpic driving force ΔH°_{rc} for the electrode reaction can be found from $\Delta H^\circ_{rc} = F(E - E^\circ) + T\Delta S^\circ_{rc}$. It is simple to show that the corresponding values of ΔH^*_i and ΔH^*_r, and ΔS^*_i and ΔS^*_r at a given electrode potential are related by[6]

$$\Delta H^*_i = \Delta H^*_r + T\Delta S^\circ_{rc} \tag{8}$$

and

$$\Delta S^*_i = \Delta S^*_r + \alpha\Delta S^\circ_{rc} \tag{9}$$

Consequently, a wealth of information on the energetics of electron transfer for *individual* redox couples ("half-reactions") can be extracted from measurements of reversible cell potentials and electrochemical rate constant-overpotential relationships, both studied as a function of temperature. Such electrochemical measurements can therefore provide information on the contributions of each redox couple to the energetics of the bimolecular homogeneous reactions which is unobtainable from ordinary chemical thermodynamics and kinetics measurements.

Relation between Electrochemical and Homogeneous Reaction Energetics

Consider the following pair of electrochemical reduction and oxidation reactions

$$Ox_1 + e^-(\text{electrode},\phi_m) \rightleftharpoons Red_1 \tag{10a}$$

$$Red_2 \rightleftharpoons Ox_2 + e^-(\text{electrode},\phi_m) \tag{10b}$$

and the corresponding homogeneous cross reaction

$$Ox_1 + Red_2 \rightleftharpoons Red_1 + Ox_2 \tag{11}$$

Providing that the interactions between the reactant and the electrode in the electrochemical transition state, and between the two reactants in the homogeneous transition state, are negligible ("weak overlap" limit), the activation barriers for reactions (10) and (11) will be closely related.

At a given value of ϕ_m (and hence electrode potential E), the thermodynamics of reactions (10) and (11) are identical since the energy required to transport the electron across the metal-solution interface in the half reactions (10a) and (10b) will then cancel. The overall activation free energy $\Delta G^*_{h,12}$ for reaction (11) can be considered to consist of separate contributions, $\Delta G^*_{h,1}$ and $\Delta G^*_{h,2}$, arising from the activation of Ox, and Red, respectively. Although a multitude of different transition-state structures may be formed, corresponding to different individual values of $\Delta G^*_{h,1}$ and $\Delta G^*_{h,2}$, the predominant reaction channel will be that corresponding to a minimum in the activation free energy $(\Delta G^*_{h,1} + \Delta G^*_{h,2})_{min}$.[10] In the "weak overlap" limit, each pair of values of $\Delta G^*_{h,1}$ and $\Delta G^*_{h,2}$ satisfying the thermodynamic constraints of reaction (11) will be identical to the corresponding pair of electrochemical free energies of activation, $\Delta G^*_{e,1}$ and $\Delta G^*_{e,2}$, for reactions (10a) and (10b), respectively, having the same transition-state structures. Therefore the energetics of reactions (10) and (11) are related in the "weak overlap" limit by

$$(\Delta G^*_{e,1} + \Delta G^*_{e,2})^E_{min} = (\Delta G^*_{h,1} + \Delta G^*_{h,2})_{min} = \Delta G^*_{h,12} \tag{12}$$

where $(\Delta G^*_{e,1} + \Delta G^*_{e,2})^E_{min}$ refers to the particular electrode potential where the sum of $\Delta G^*_{e,1}$ and $\Delta G^*_{e,2}$ is a minimum. Although only the sum $(\Delta G^*_{h,1} + \Delta G^*_{h,2})_{min}$ can be determined experimentally for a given homogeneous reaction, the values of $\Delta G^*_{e,1}$ and $\Delta G^*_{e,2}$ may be examined individually as a function of the free energy driving forces ΔG°_1 and ΔG°_2 for these two half reactions (10a) and (10b), which equal $F(E - E^\circ_1)$ and $F(E - E^\circ_2)$, respectively, where E°_1 and E°_2 are the corresponding standard electrode potentials.

This relationship is illustrated schematically in Fig. 1. Curves 11' and 22' represent plots of ΔG^*_e against the reaction free energy $F(E - E^\circ)$ for a pair of cathodic and anodic half reactions on a common scale of electrode potential FE; such curves are generally expected to be curved in the manner shown (*vide infra*) so that a shallow minimum in the plot of $(\Delta G^*_{e,1} + \Delta G^*_{e,2})$ versus FE will be obtained. In practice, unless ΔG^*_e is small ($\lesssim$ 3-4 kcal mol^{-1}) the slopes of these plots, i.e., the cathodic and anodic transfer coefficients, are often found to be equal and close to 0.5 so that to a good approximation[11-13]

$$2\Delta G^*_{e,12} = \Delta G^*_{h,12} \tag{13}$$

where $\Delta G^*_{e,12}$ is the value of ΔG^*_e at the intersection of the $\Delta G^*_{e,1}$ - E and $\Delta G^*_{e,2}$ - E plots.

For the special case where the cathodic and anodic half-reactions are identical, since the two ΔG^*_e - E plots must intersect at E° for the redox couple, then Eqn. (13) can be written in terms of the electrochemical and homogeneous intrinsic barriers:

$$2\Delta G^*_{ie} = \Delta G^*_{ih} \tag{14}$$

Relationships having the same form as Eqn. (14) can also be written for the enthalpic and entropic contributions to the intrinsic free energy barriers.[10]

Provided that the reactions are adiabatic and the conventional collision model applies, Eqn. (14) can be written in the familiar form relating the rate constants of electrochemical exchange and homogeneous self-exchange reactions:[14]

$$\left(\frac{k^{s}_{corr}}{Z_e}\right)^2 = \left(\frac{k^{h,ex}_{corr}}{Z_h}\right) \qquad (15)$$

where $k^{h,ex}_{corr}$ is the (work-corrected) rate constant for homogeneous self exchange, and Z_e and Z_h are the electrochemical and homogeneous collision frequencies, respectively.

In the following sections, we shall explore the applicability of such relationships to experimental data for some simple outer-sphere reactions involving transition-metal aquo complexes. In keeping with the distinction between intrinsic and thermodynamic barriers [Eqn. (7)], exchange reactions will be considered first, followed by a comparison of driving force effects for related electrochemical and homogeneous reactions.

Electron Exchange

Tables I and II contain electrochemical kinetics and related thermodynamics parameters for several transition-metal redox couples gathered at the mercury-aqueous interface. These systems were selected since the kinetics can be measured accurately under experimental conditions where the diffuse-layer potentials ϕ_d are small and/or could be estimated with confidence, yielding trustworthy estimates of k^{s}_{corr} from the observed values k^{s}_{ob} [Eqn. (5)]. (Details are given in references 11 and 15.) Also, the observed rates probably refer to outer-sphere pathways, and the rate constants for the corresponding homogeneous self-exchange reactions are available, or can be estimated from rate data for closely related cross reactions.[16] These latter values, $k^{h,ex}_{corr}$, which are also corrected for electrostatic work terms[16] are given

alongside in Table I for comparison. Also included are estimates of $k_{corr}^{h,ex}$, $k_{corr}^{h,ex}(calc)$, that were obtained from the corresponding values of k_{corr}^{s} using Eqn. (15). [Values of 5×10^3 cm s^{-1} and 2×10^{11} $\underline{M}^{-1}$ s^{-1} were employed for Z_e and Z_h, respectively, appropriate for a "typical" reactant mass of 200 and radius 3.5 Å.[17]]

It is seen that the values of $k_{corr}^{h,ex}$ for the five aquo couples in Table I are uniformly larger than the corresponding values of $k_{corr}^{h,ex}(calc)$ by typically 1-2 orders of magnitude, although the value of $k_{corr}^{h,ex}$ for $Fe_{aq}^{3+/2+}$ (where "aq" denotes aquo ligands) is over 10^5-fold larger than $k_{corr}^{h,ex}(calc)$. Such discrepancies have been discussed previously.[11] The most general derivation of Eqn. (14) [and hence Eqn. (15)] involves the assumption that the stabilization of the electrochemical transition state resulting from the proximity of the reactant to the electrode surface will equal one half of the corresponding stabilization of the homogeneous transtion state arising from the approach of the two reactants.[14] In terms of the conventional model, this will occur when the distance R^h between the homogeneous reactants equals the distance R^e between the heterogeneous reactant and its electrostatic image in the electrode.[14] The observation that $k_{12}^{h,ex} > k_{12}^{h,ex}(calc)$, and hence $2\Delta G_{ie}^{*} > \Delta G_{ih}^{*}$, is expected for electrochemical outer-sphere reactions on this basis since the reactant plus coordinated ligands will be separated from the electrode surface by the "inner layer" of solvent molecules (i.e. the electrode's "coordination layer") so that generally $R^e > R^h$. From the rate responses for Cr_{aq}^{3+} and Eu_{aq}^{3+} reduction at the mercury-aqueous interface to systematic variations in the double-layer structure, it has been concluded that at least two, and possibly three, water molecules lie between the electrode surface and the metal cations in the transition state.[18]

Additional insight can be obtained by comparing the electrochemical and homogeneous activation parameters. Table II contains values of $2\Delta G_{ie}^{*}$, $2\Delta H_{ie}^{*}$,

and $2\Delta S^*_{ie}$ for three aquo couples [$V^{3+/2+}_{aq}$, $Eu^{3+/2+}_{aq}$, and $Cr^{3+/2+}_{aq}$] for which work term corrections can be reliably made as a function of temperature.[8] The values of ΔG^*_{ie} were obtained from the corresponding values of k^s_{corr} using Eqn. (6), assuming that the frequency factor A equals Z_e (5×10^3 cm s^{-1}). The intrinsic enthalpies of activation ΔH^*_{ie} were obtained from the slope of a plot of $-R(\ln k^s_{corr} - \ln T^{1/2})$ versus $1/T$,[8] and the corresponding intrinsic entropies of activation ΔS^*_{ie} from $\Delta S^*_{ie} = (\Delta H^*_{ie} - \Delta G^*_{ie})/T$. Table II also contains the intrinsic free energies (ΔG^*_{ih}), enthalpies (ΔH^*_{ih}), and entropies of activation (ΔS^*_{ih}) for the corresponding homogeneous self-exchange reactions. These were similarly obtained from the work-corrected homogeneous rate constants. (See refs. 16 and 17 for calculational details and data sources).

Comparison of the corresponding electrochemical and homogeneous reorganization parameters reveal that $2\Delta G^*_{ie} > \Delta G^*_{ih}$, which follows from the observation that $k^{h,ex}_{corr} > k^{h,ex}_{corr}(calc)$ [Eqn. (14)]. This inequality in free energies is paralleled by greater differences between $2\Delta H^*_{ie}$ and ΔH^*_{ih}, these being partially compensated by values of $2\Delta S^*_{ie}$ that are significantly less negative than ΔS^*_{ih}. The classical model of outer-sphere electron transfer predicts that both ΔS^*_{ie} and ΔS^*_{ih} should be close to zero (within ca. 1 e.u.).[11,19] Part, but probably not all, of the observed values of ΔS^*_{ih} can be ascribed to the influence of nuclear tunneling and nonadiabaticity;[19] these factors may account entirely for the observed small negative values of ΔS^*_{ie}. The larger negative values of ΔS^*_{ih} may arise partly from the solvent ordering that probably attends the formation of the highly charged precursor complex from the separated cationic reactants.[16] Nevertheless, by and large the relative values of the electrochemical and homogeneous reorganization parameters are reasonably close to the expectations of the weak overlap model.[14] The observed differences are consistent with the anticipated smaller extent of the reactant-electrode interactions as compared

with the homogeneous reactant-reactant interactions in the transition states for electron transfer.

The remaining four redox couples in Table I, containing amine and related ligands, exhibit values of $k_{corr}^{h,ex}$ that are very different from the corresponding electrochemical estimates $k_{corr}^{h,ex}(calc)$. Similar discrepancies between the experimental results and the predictions of Eqn. (15) have been observed previously,[20,21] although corrections for work terms have seldom been made. A puzzling feature of these data is the relatively small variations in k_{corr}^{s} and hence $k_{corr}^{h,ex}(calc)$ for the three Co(III)/(II) couples compared with $k_{corr}^{h,ex}$. These discrepancies may arise from differences in electronic transmission coefficients at the electrode surface and in the bulk solution,[20] from additional contributions to the work terms not considered in the Debye-Hückel and/or Gouy-Chapman models, or from unexpected differences in the outer-shell reorganization energies in the surface and bulk environments.[11]

Electrochemical and homogeneous reorganization parameters for $Co(en)_3^{3+/2+}$ are also given in Table II. The large disparity between the electrochemical and homogeneous parameters is highlighted by a value of ΔH_{ie}^{*} that is close to zero. Since the inner-shell contribution to ΔH_{ie}^{*} is undoubtedly large ($\geq$5 kcal mol^{-1}), this result indicates that the electrode is markedly influencing the transition-state structure. We have also obtained comparable electrochemical reorganization parameters for the $Co(NH_3)_6^{3+/2+}$ couple. Since there is strong evidence that ammine complexes can approach the electrode surface more closely than the more strongly solvated aquo complexes,[18] it seems likely that this unexpected electrochemical behavior of $Co(en)_3^{3+/2+}$ arises from a specific influence of the interfacial environment.

Influence of Thermodynamic Driving Force

Given that the reorganization parameters for electrochemical exchange of various aquo redox couples are in acceptable agreement with the corresponding homogeneous rate parameters on the basis of the weak overlap model, it is of interest to compare the manner in which the energetics of these two types of redox processes respond to the application of a net thermodynamic driving force.

For one-electron electrochemical reactions, the harmonic oscillator ("Marcus") model[22] yields the following predicted dependence of ΔG_e^* upon the electrode potential:

$$\Delta G_e^* = \Delta G_{ie}^* \pm 0.5\, F(E - E^\circ) + \frac{F(E-E^\circ)^2}{16\Delta G_{ie}^*} \qquad (16)$$

where the plus/minus sign refers to reduction and oxidation reactions, respectively. The transfer coefficient α [Eqn. (7)] is therefore predicted to decrease linearly from 0.5 with increasing electrochemical driving force $\pm F(E - E^\circ)$. The derivation of Eqn. (16) involves the assumption that the reactant and product free energy barriers are parabolic and have identical shapes, and that the reactions are adiabatic yet involve only a small "resonance splitting" of the free energy curves in the intersection region.[22]

A number of experimental tests of Eqn. (16) have been made.[15,23] Generally speaking, it has been found that $\alpha \approx 0.5$ at small to moderate overpotentials, in agreement with Eqn. (16). Tests of this relation over sufficiently large ranges of overpotential where the quadratic term becomes significant are not numerous. A practical difficulty with multicharged redox couples is that the extent of the work term corrections is frequently sufficiently large to make the extraction of k_{corr}, and hence ΔG_e^* and α, from the observed rate-potential behavior fraught with uncertainty. However, we have recently obtained

kinetic data for Cr^{2+}_{aq}, Eu^{2+}_{aq} and V^{2+}_{aq} electrooxidation over wide ranges of anodic overpotential (up to 900 mv) under conditions where the electrostatic work terms are small.[15] The anodic transfer coefficients α_a for all those reactions were found to decrease with increasing anodic overpotential, but to a greater extent than predicted by Eqn. (16). This behavior contrasts that found for cathodic overpotentials, where the cathodic transfer coefficients α_c remain essentially constant at 0.5, even over regions of overpotential where detectable decreases in α_c are predicted by Eqn. (16).[15,24] These aquo redox couples therefore exhibit a markedly different overpotential dependence of the anodic and cathodic rate constants; this contrasts with the symmetrical dependence predicted by Eqn. (16). An example of this behavior is shown in Fig. 2 which is a plot of ΔG^*_e versus $(E - E^\circ)$ for $Cr^{3+/2+}_{aq}$ at the mercury-aqueous interface at both anodic and cathodic overpotentials. The solid curves are obtained from the experimental data, and the dashed lines show the overpotential dependence of ΔG^*_e predicted from Eqn. (16).

The prediction corresponding to Eqn. (16) for driving force effects upon homogenous kinetics is[22]

$$\Delta G^*_{h,12} = \Delta G^*_{ih,12} + 0.5\ \Delta G^\circ_{12} + \frac{(\Delta G^\circ_{12})^2}{16\Delta G^*_{ih,12}} \qquad (17)$$

where $\Delta G^*_{ih,12}$ is the mean of the intrinsic barriers for the parent self-exchange reactions $[0.5(\Delta G^*_{ih,1} + \Delta G^*_{ih,2})]$ and ΔG°_{12} is the free energy driving force for the cross reaction. Equation (17) has been found to be in satisfactory agreement with experimental data for a number of outer-sphere cross reactions having small or moderate driving forces. However there appear to be significant discrepancies for some reactions having large driving forces (where the last term in Eqn. (17) becomes important) in that the rate constants do not increase with increasing driving force to the extent predicted by Eqn. (17); i.e. the

values of $\Delta G^*_{h,12}$ are larger than those calculated from the corresponding values of $\Delta G^*_{ih,12}$ and ΔG°_{12} using Eqn. (17).[16,25-27]

It has been suggested that these apparent discrepancies could be due to the values of $\Delta G^*_{h,12}$ and $\Delta G^*_{ih,12}$ that are obtained from the experimental work-corrected rate constants being incorrectly large due to nonadiabatic pathways,[25-27] or to the presence of additional unfavorable work terms arising from solvent orientation required to form the highly charged precursor complex.[16] An alternative, or additional, explanation is that the free energy barriers are anharmonic so that the quadratic driving force dependence of Eqn. (17) is inappropriate. It is interesting to note that the form of the discrepancies between the kinetics data for the electrooxidation of aquo cations and Eqn. (16) is at least qualitatively similar in that both involve unexpectedly small dependencies of the rate constants upon the thermodynamic driving force. Moreover, the large majority of homogeneous reactions for which such discrepancies have been observed involve the oxidation of aquo cations.[16,25] However, nonadiabaticity effects cannot explain the asymmetry between the ΔG^*_e - E plots at anodic and cathodic overpotentials (Fig. 2). Also, any specific work term effects should be different (and probably smaller) at the mercury-aqueous interface compared with homogeneous reactions between multicharged cations,[11] yet any anharmonicity of the free energy barriers should be similar, at least on the basis of the weak overlap model. A quantitative comparison of the driving force dependence of the kinetics of related electrochemical and homogeneous reactions should therefore shed light on the causes of the observed discrepancies for the latter, more complicated processes.

One can generally express the free energy barriers ΔG^*_e for the pair of cathodic and anodic electrochemical reactions (10a) and (10b) as [cf. Eqns. (7) and (16)]:

$$\Delta G^{*}_{e,1} = \Delta G^{*}_{ie,1} + \alpha_1 \Delta G^{\circ}_{1} \tag{18a}$$

and

$$\Delta G^{*}_{e,2} = \Delta G^{*}_{ie,2} + \alpha_2 \Delta G^{\circ}_{2} \tag{18b}$$

where α_1 and α_2 are the transfer coefficients for these two reactions at a given electrode potential. A similar relationship may be written for the free energy barrier $\Delta G^{*}_{h,12}$ of the corresponding homogeneous cross reaction (11) [cf. Eqn. (17)]:

$$\Delta G^{*}_{h,12} = \Delta G^{*}_{ih,12} + \alpha_{12} \Delta G^{\circ}_{12} \tag{19}$$

where α_{12} is a "chemical" transfer coefficient. Although α_1 and α_2 are determined only by the shapes of the free energy barriers for the individual redox couples at a given driving force, α_{12} is a composite quantity which is determined not only by both α_1 and α_2 but also by the relative magnitudes of $\Delta G^{*}_{ih,1}$, $\Delta G^{*}_{ih,2}$ and $\Delta G^{*}_{h,12}$.

Nevertheless, comparison of values of $\Delta G^{*}_{h,12}$ for a series of related cross reactions having systematically varying driving forces can yield useful information. Figure 3 is a plot of $\Delta G^{*}_{h,12}/\Delta G^{*}_{ih,12}$ versus $\Delta G^{\circ}_{12}/\Delta G^{*}_{ih,12}$ for a series of cross reactions involving the oxidation of various aquo complexes. (The values of ΔG^{*}_{12} and $\Delta G^{*}_{ih,12}$ were obtained from the measured homogeneous rate constants in the same way as the homogeneous free energies of activation given in Tables I and II. Details are given in ref. 16.) The graphical presentation in Fig. 3 has the virtue that the values of $\Delta G^{*}_{h,12}$ for different cross reactions are normalized for variations in the intrinsic barriers $\Delta G^{*}_{ih,12}$; the driving force dependence of $\Delta G^{*}_{h,12}$ predicted by the Marcus model all fall on a common curve (shown as a solid line in Fig. 3) when presented in this manner.[28] [Omitted

from Fig. 3 are reactions involving $Co_{aq}^{3+/2+}$ since there is evidence that the measured self-exchange rate does not correspond to an outer-sphere pathway.[29] It is seen that the experimental points deviate systematically from the Marcus predictions in that the apparent values of α_{12} [Eqn. (19)] are significantly smaller than predicted from Eqn. (17) at moderate to high driving forces. Figure 4 consists of the same plot as Fig. 3 but for a number of outer-sphere cross reactions involving reductants other than aquo complexes.[28] In contrast to Fig. 3, reasonable agreement with the Marcus prediction is obtained (cf. ref. 28). The data in Fig. 3 are also shown in Fig 5 as a plot of $[\Delta G_{12}^{*} - \Delta G_{i,12}^{*}]$ versus $-[0.5\Delta G_{12}^{\circ} + (\Delta G_{12}^{\circ})^2/16\Delta G_{i,12}^{*}]$. Since this plot is an expression of Eqn. (17), the Marcus model predicts a slope of unity (the solid line in Fig. 5). However, the points are almost uniformly clustered beneath this predicted line, and increasingly so as $-\Delta G_{12}^{\circ}$ increases, again indicating that α_{12} tends to be smaller than predicted.

It therefore seems feasible that these anomalously small values of α_{12} noted from Figs. 3 and 5 have their primary origin in the oxidation half-reactions which uniformly involve aquo complexes. This possibility was explored by converting the electrooxidation data into a form suitable for direct comparison with the homogeneous data in Fig. 5 in the following manner. As noted above, the free energy barrier $\Delta G_{h,12}^{*}$ for each outer-sphere cross section will consist of contributions $\Delta G_{h,1}^{*}$ and $\Delta G_{h,2}^{*}$ from the oxidant and reductant, respectively. In the "weak overlap" limit $\Delta G_{h,1}^{*}$ and $\Delta G_{h,2}^{*}$ will equal the free energy barriers $\Delta G_{e,1}^{*}$ and $\Delta G_{e,2}^{*}$ for the corresponding electrochemical reactions at an electrode potential where the sum $(\Delta G_{e,1}^{*} + \Delta G_{e,2}^{*})$ is a minimum [Eqn. (12) and Fig. 1]. Estimates of $\Delta G_{h,2}^{*}$ for Eu_{aq}^{2+}, Cr_{aq}^{2+}, and V_{aq}^{2+} oxidation as a function of the half-reaction driving force $\Delta G_2^{\circ}[= -F(E - E_2^{\circ})]$ were obtained from the corresponding ΔG_e^{*} - E plots (see Fig. 2 and ref. 15) by assuming that they have the same shape

but replacing the value of ΔG^*_e at $\Delta G^\circ_2 = 0$ (i.e. ΔG^*_{ie}) by $0.5\Delta G^*_{ih}$. [This procedure corrects for the differences between ΔG^*_{ie} and $0.5\Delta G^*_{ih}$ (Table II) resulting from the limitations of the weak overlap model (Eqn. (14))]. The accompanying plots of $\Delta G^*_{h,1}$ versus ΔG°_1 for the reduction half reactions involved in Fig. 5 were constructed using the experimental value of $\Delta G^*_{ih,12}$ by assuming that the harmonic oscillator model applies, i.e. by utilizing Eqn. (16) written for homogeneous half reactions:

$$\Delta G^*_{h,1} = 0.5\Delta G^*_{ih,12} + 0.5\Delta G^\circ_1 + (\Delta G^\circ_1)^2/8\Delta G^*_{ih,12} \qquad (20)$$

These pairs of $\Delta G^*_{h,1} - \Delta G^\circ_1$ and $\Delta G^*_{h,2} - \Delta G^\circ_2$ curves were plotted on a common driving force (i.e. electrode potential) axis such that $\Delta G^\circ_1 - \Delta G^\circ_2 = \Delta G^\circ_{12}$, and the required estimates of $\Delta G^*_{h,12}$ for each cross reaction were then obtained from the sum $(\Delta G^\circ_{h,1} + \Delta G^\circ_{h,2})$ at the value of ΔG° where the quantity has a minimum value [Eqn. (12)]. These estimates of $\Delta G^*_{h,12}$ are plotted as open symbols in Fig. 5 for the reactions having moderate to large driving forces ($-\Delta G^\circ_{12} > 8$ kcal mol^{-1}), alongside the corresponding experimental values of $\Delta G^*_{h,12}$. It is seen that the estimated values of $\Delta G^*_{h,12}$ diverge from the straight line predicted from the harmonic oscillator model to a similar, albeit slightly smaller, extent than the experimental values. Admittedly, there is no particular justification for assuming that the reduction half reactions obey the harmonic oscillator model. However, it turns out that the estimates of $\Delta G^*_{h,12}$ are relatively insensitive to alterations in the shapes of the $\Delta G^*_{h,1} - \Delta G^\circ_1$ plots. It therefore seems reasonable that the deviations of the activation free energies for highly exoergic electrochemical and homogeneous reactions illustrated in Figs. 2 and 5 may arise partly from the same source, i.e. from values of α_2 for the oxidation half reactions that are unexpectedly small. That is not to say that other factors are not responsible, at least in part, for these discrepancies. Nonadiabaticity, work terms, specific solvation,

and other environmental effects may all play important roles depending on the reactants. For example, there is evidence to suggest that the true rate constant for outer-sphere $Fe_{aq}^{3+/2+}$ self-exchange is significantly smaller than the directly measured value;[30] this can account for a good part of the unexpectedly slow rates of cross reactions involving this couple.

It remains to consider possible reasons for these apparent deficiencies of the harmonic oscillator model for the oxidation of aquo cations. Some discussion of the electrochemical results has been given previously.[15] It was concluded that the most likely explanation for the observed disparities between the experimental results and the predictions of Eqn. (16) (Fig. 2) is that the reactant and product free energy barriers for the aquo redox couples have markedly different shapes.[13] Such an asymmetry of the free energy barriers is unlikely to arise from inner-shell (metal-ligand vibrational) contributions, at least within the confines of a classical model. Thus choosing even unreasonably large differences in vibrational force constants for the oxidized and reduced forms generates much smaller differences in the shapes of the resulting anodic and cathodic Tafel plots than are observed experimentally (Fig. 2).[15] Indeed, such calculations performed for homogeneous reactions led to an earlier assertion that anharmonicity effects were unlikely to account for the extent of the observed breakdowns in the applicability of the Marcus cross relationship [Eqn. (17)] as exemplified in Figs. 3 and 5.[25] A plausible, albeit somewhat inaccessible, source of asymmetry in the free energy barriers could lie in major differences in short-range solvent structure between the reduced and oxidized aquo complexes. There is strong evidence that tripositive aquo complexes induce extensive solvent ordering via field-assisted hydrogen bonding with the aquo ligands, which is partly dissipated upon reduction to the dipositive species.[31,32] This short-range reorientation of water

molecules may well contribute unequally to the individual free energy curves for the oxidized and reduced species, thereby generating the required nonsymmetry. A related point is that the reactant and product *potential*-energy barriers will be highly nonsymmetrical even when the *free*-energy driving force ΔG°_{rc} is zero (i.e. at E°), as a result of the especially large positive values of ΔS°_{rc} for the aquo redox couples (Table I). Thus the electrooxidation reactions will be highly exothermic ($-\Delta H^\circ_{rc} \approx 15$ kcal mol^{-1}) even when $\Delta G^\circ_{rc} = 0$, and increasingly so at anodic overpotentials. In contrast, the electroreduction reactions are endothermic ($\Delta H^\circ_{rc} > 0$) within the entire overpotential range that is accessible to experiment.

Conclusions

It seems clear that kinetics as well as thermodynamics data gathered for simple electrode reactions can contribute significantly towards the development of our fundamental understanding of electron transfer in condensed media. In particular, detailed studies of electrochemical kinetics with due regard for work term corrections can yield information on the shapes of free energy barriers, and also their enthalpic and entropic components, that are largely inaccessible from studies of homogeneous redox kinetics. The former can provide a direct means of detecting deficiencies in the applicability of the harmonic oscillator model which forms the kernel of most contemporary treatments of electron transfer.

Experimental comparisons between the kinetics of related electrochemical and homogeneous reactions in suitable cases can also yield insights into the differences as well as similarities between these two major types of redox processes.[3,11,33] Unfortunately, there is still a paucity of electrochemical kinetics data on substrates other than mercury. However, recent advances in the methods for preparing and characterizing clean metal surfaces, particularly

for single crystals, should allow the acquisition of quantitative data for a much wider range of reactions and surface environments than hitherto available. It is hoped that a greater comparison of results for heterogeneous and homogeneous processes will occur in the future; this should be to the benefit of both areas.

Acknowledgements

We are grateful to Prof. John Endicott for sending us a copy of ref. 29 prior to publication. This work is supported in part by the Air Force Office of Scientific Research and the Office of Naval Research.

References and Notes

1. R.A. Marcus, J. Phys. Chem. 72, 891 (1968).
2. N. Sutin, Acc. Chem. Res. 1, 225 (1968).
3. M.J. Weaver, Inorg. Chem. 18, 402 (1979).
4. R. Parsons, Croat. Chim. Acta 42, 281 (1970).
5. M. Temkin, Zh. Fiz. Khim. 22, 1081 (1948).
6. M.J. Weaver, J. Phys. Chem. 80, 2645 (1976).
7. M.J. Weaver, Israel J. Chem. 18, 35 (1979).
8. M.J. Weaver, J. Phys. Chem. 83, 1748 (1979).
9. E.L. Yee, R.J. Cave, K.L. Guyer, P.D. Tyma, M.J. Weaver, J. Am. Chem. Soc. 101, 1131 (1979).
10. T.W. Newton, J. Chem. Educ. 45, 571 (1968).
11. M.J. Weaver, J. Phys. Chem. 84, 568 (1980).
12. M.J. Weaver, Inorg. Chem. 15, 1733 (1976).
13. In the Appendix to reference (11), Eqn. (13) was claimed to be generally applicable in the "weak overlap" limit when $\Delta G^*_{e,1}$ and $\Delta G^*_{e,2}$ exhibit a quadratic dependence upon $(E - E^\circ)$ as predicted by the harmonic oscillator model.[1] In fact, the proof given is not entirely correct inasmuch as the energy minimization condition $[\partial(\Delta G^*_{e,1} + \Delta G^*_{e,2})/\partial\beta = 0]$ employed in

ref. 11 leads to Eqn. (12), Eqn. (13) only being obtained as a special case when the slopes of the $\Delta G^*_{e,1}$ - E and $\Delta G^*_{e,2}$ - E plots are equal and of opposite sign at the intersection point.

14. R.A. Marcus, J. Phys. Chem. 67, 853 (1963).

15. P.D. Tyma, M.J. Weaver, J. Electroanal. Chem. 111, 185 (1980).

16. M.J. Weaver, E.L. Yee, Inorg. Chem. 19, 1936 (1980).

17. The estimate of Z_h given in refs. 10 and 14 (6×10^{10} $M^{-1}s^{-1}$) is incorrect due to calculational error.

18. M.J. Weaver, T.L. Satterberg, J. Phys. Chem. 81, 1772 (1977).

19. B.S. Brunschwig, J. Logan, M.D. Newton, N. Sutin, J. Am. Chem. Soc. 102, 5798 (1980).

20. J.F. Endicott, R.R. Schroeder, D.H. Chidester, D.R. Ferrier, J. Phys. Chem. 77, 2579 (1973).

21. T. Saji, T. Yamada, S. Aoyagui, J. Electroanal. Chem. 61, 147 (1975); T. Saji, Y. Mariyama, S. Aoyagui, *ibid*, 86, 219 (1978).

22. R.A. Marcus, J. Chem. Phys. 43, 679 (1965).

23. See ref. 15 for references to earlier work.

24. M.J. Weaver, F.C. Anson, J. Phys. Chem. 80, 1861 (1976).

25. M. Chou, C. Creutz, N. Sutin, J. Am. Chem. Soc. 99, 5615 (1977).

26. G.M. Brown, H.J. Krentzien, M. Abe, H. Taube, Inorg. Chem. 18, 3374 (1979).

27. V. Balzani, F. Scandola, G. Orlandi, N. Sabbatini, M.T. Indelli, J. Am. Chem. Soc. 103, 3370 (1981).

28. J.F. Endicott, B. Durham, M.D. Glick, T.J. Anderson, J.M. Kuszaj, W.G. Schmonsees, K.P. Balakishnan, J. Am. Chem. Soc. 103, 1431 (1981).

29. J.F. Endicott, B. Durham, K. Kumar, Inorg. Chem. in press.

30. J.T. Hupp, M.J. Weaver, to be submitted for publication.

31. E.L. Yee, R.J. Cave, K.L. Guyer, P.D. Tyma, M.J. Weaver, J. Am. Chem. Soc. 101, 1131 (1979).

32. M.J. Weaver, S.M. Nettles, Inorg. Chem. 19, 1641 (1980).

33. For example, see K.L. Guyer, S.W. Barr, R.J. Cave, M.J. Weaver, in "Proc. 3rd Symp. on Electrode Processes", S. Bruckenstein, J.D.E. McIntyre, B. Miller, E. Yeager (eds), Electrochemical Society, Princeton, NJ, 1980, p. 390.

TABLE I - Rate Constants and Thermodynamic Parameters for Selected Electrochemical Exchange and Homogeneous Self-Exchange Reactions at 25°C.

Redox Couple	E^f [a] mV vs. s.c.e.	ΔS°_{rc} [b] cal deg^{-1} mol^{-1}	k^s_{corr} [c] cm s^{-1}	$k^{h,ex}_{corr}$ [d] M^{-1}s^{-1}	$k^{h,ex}_{corr(calc)}$ [e] M^{-1} s^{-1}
$Ru(OH_2)_6^{3+/2+}$	-15 (0.3)	36	2×10^{-2}	200	3
$V(OH_2)_6^{3+/2+}$	-475 (0.2)	37	1×10^{-3}	3×10^{-2}	8×10^{-3}
$Fe(OH_2)_6^{3+/2+}$	500 (0.2)	43	$\sim 1 \times 10^{-4}$	15	8×10^{-5}
$Eu(OH_2)_n^{3+/2+}$	-625 (0.2)	48	8×10^{-5}	4×10^{-4}	5×10^{-5}
$Cr(OH)_6^{3+/2+}$	-660 (1)	49	2×10^{-6}	2×10^{-6}	3×10^{-8}
$Ru(NH_3)_6^{3+/2+}$	-180 (0.2)	18	$\gtrsim 10$	5×10^{4}	$\gtrsim 8 \times 10^{5}$
$Co(en)_3^{3+/2+}$ [j]	-460 (1)	37	5 10^{-2} [f]	2.5×10^{-4}	20
$Co(bpy)_3^{3+/2+}$ [k]	70 (0.05)	22	~ 5 10^{-4} [f]	~ 80	2×10^{-3}
$Co(EDTA)^{-/2-}$	135 (0.5) [i]	-8 [i]	~ 5 10^{-2} [g]	$\sim 1 \times 10^{-6}$ [h]	20

[a] Formal potential of redox couple, determined at ionic strength noted in parentheses. Data from ref. 9 unless otherwise indicated.

[b] Reaction entropy of redox couple, determined at same ionic strength as E^f. Data from ref. 9 unless otherwise indicated.

[c] Standard rate constant for redox couple measured in 0.1-0.4 M KPF_6 and/or $NaClO_4$ supporting electrolytes, corrected for electrostatic double-layer effect using Eqn. (5) assuming that $\phi_{rp} = \phi_d^{GC}$. Kinetic data from ref. 10 unless otherwise stated.

[d] Rate constant for homogeneous self exchange, corrected for electrostatic work terms using Debye-Hückel-Bronsted model. Data taken from sources quoted in ref. 14 unless otherwise stated.

Notes to Table I Continued.

[e] Rate constant for homogeneous self exchange, calculated from corresponding value of k^s_{corr} using Eqn. (14), assuming that $Z_e = 5 \times 10^3$ cm s^{-1}, and $Z_h = 2 \times 10^{11}$ $\underline{M}^{-1}$ s^{-1} (see text).

[f] S. Sahami, J. Farmer, M.J. Weaver, unpublished results.

[g] N. Tanaka, A. Yamada, Electrochim. Acta 14, 491 (1969).

[h] Quoted in R.G. Wilkins, R.E. Yelin, Inorg. Chem. 7, 2667 (1968).

[i] [j] E.L. Yee, M.J. Weaver, unpublished results.

[k] en = ethylenediamine.

bpy = 2,2'-bipyridine.

Table II - Comparison between Experimental Reorganization Parameters for some Electrochemical and Homogeneous Exchange Reactions.

Redox Couple	$2\Delta G^*_{ie}$ [a] kcal mol^{-1}	$2\Delta H^*_{ie}$ [b] kcal mol^{-1}	$2\Delta S^*_{ie}$ [c] cal deg^{-1} mol^{-1}	ΔG^*_{ih} [d] kcal mol^{-1}	ΔH^*_{ih} [e] kcal mol^{-1}	ΔS^*_{ih} [f] cal deg^{-1} mol^{-1}
$V(OH_2)_6^{3+/2+}$	18.2	16.5	-5.5	17.5	13.0	-15
$Eu(OH_2)_6^{3+/2+}$	21.2	17.2	-9	20.0	~15.5	(-15)
$Cr(OH_2)_6^{3+/2+}$	25.6	23.4	-7.5	23.2	~18.5	(-15)
$Co(en)_3^{3+/2+}$	13.6	~0 [g]	-45	20.3	13.8	-22

[a] Twice the intrinsic electrochemical free energy of activation, obtained from value of k^s_{corr} at mercury-aqueous interface given in Table I using $\Delta G^*_{ie} = -RT \ln(k^s_{corr}/Z_e)$, where $Z_e = 5 \times 10^3$ cm s^{-1}.

[b] Twice the intrinsic electrochemical enthalpy of activation, obtained from $H^*_{ie} = -R[d(\ln k^s_{corr} - \ln T^{\frac{1}{2}})/d(1/T)]$ (see text). See refs. 8 and 10 for original data, except where indicated.

[c] Twice the intrinsic electrochemical entropy of activation, obtained from $2\Delta S^*_{ie} = 2\Delta H^*_{ie} - 2\Delta G^*_{ie}$.

[d] Intrinsic free energy of activation for homogeneous self-exchange, obtained from values of $k^{h,ex}_{corr}$ given in Table I using $\Delta G^*_{ih} = -RT \ln(k^{h,ex}_{corr}/Z_h)$, where $Z_h = 2 \times 10^{11}$ $\underline{M}^{-1}$ s^{-1}.

[e] Intrinsic enthalpy of activation for homogeneous self-exchange. Values for $V^{3+/2+}_{aq}$ and $Co(en)^{3+/2+}_3$ obtained experimentally (see ref. 14 for sources and calculational details). Values for $Eu^{3+/2+}_{aq}$ and $Cr^{3+/2+}_{aq}$ obtained from ΔG^*_{ih} assuming that $\Delta S^*_{ih} = -15$ e.u.

[f] Intrinsic entropy of activation for homogeneous self-exchange. Values for $V^{3+/2+}_{aq}$ and $Co(en)^{3+/2+}_3$ obtained from ΔG^*_{ih} and ΔH^*_{ih}. Values in parentheses are estimates, based on the observation that $\Delta S^*_{ih} \approx -15$ e.u. for several related aquo redox couples.[16]

[g] J. Farmer, M.J. Weaver, unpublished results.

Figure Captions

Figure 1

Schematic illustration of general relationship between electrochemical and homogeneous redox reaction energetics. Curves 11' and 22' are plots of activation free energy ΔG_e^* versus thermodynamic driving force -FE for an electroreduction and electrooxidation reaction [reactions (10a) and (10b)], respectively. E_1°, and E_2° are the standard electrode potentials for these two redox couples. Curve 33' is formed by the sum $(\Delta G_{e,1}^* + \Delta G_{e,2}^*)^E$. The corresponding homogeneous activation barrier $\Delta G_{h,12}^*$ is, in the "weak overlap" limit, given by the minimum in this curve [Eqn. (12)].

Figure 2

The electrochemical free energy of activation ΔG_e^* for $Cr(OH_2)_6^{3+/2+}$ at the mercury-aqueous interface, plotted against the electrode potential for both anodic and cathodic overpotentials. Solid lines are obtained from the experimental rate constant-overpotential plot in ref. 12, using Eqn. (6) [assuming $A = 5 \times 10^3$ cm·s^{-1}]. Dashed lines are the predictions from Eqn. (16).

Figure 3

Plot of $\Delta G_{12}^*/\Delta G_{i,12}^*$ against $-\Delta G_{12}^\circ/\Delta G_{i,12}^*$ for homogeneous cross reactions involving oxidation of aquo cations. Key to oxidants and data sources: 1-10 are tabulated in ref. 16. 1. Fe_{aq}^{3+}; 2. Ru_{aq}^{3+}; 3. Np_{aq}^{4+}; 4. V_{aq}^{3+}; 5. Eu_{aq}^{3+}; 6. $Ru(NH_3)_6^{3+}$; 7. $Ru(NH_3)_5py^{3+}$; 8. $Co(en)_3^{3+}$; 9. $Co(phen)_3^{3+}$; 10. $Co(bpy)_3^{3+}$; 11. $Ru(NH_3)_5isn^{3+}$, ref. 26; 12. $Co(phen)_3^{3+}$, ref. 25; 13. $Co(phen)_3^{3+}$, T.J. Przystas and N. Sutin, J. Am. Chem. Soc. 95, 5545 (1973); 14 to 17 and 25 are from W. Böttcher, G.M. Brown and N. Sutin, Inorg. Chem. 18, 1447 (1979); 14. $Co(phen)_3^{3+}$; 15. $Ru(NH_3)_5isn^{3+}$; 16. $Os(bpy)_3^{3+}$; 17. $Ru(bpy)_3^{3+}$; 18 to 22 are from C. Creutz, Inorg. Chem. 17, 1056 (1978); 18. $*Ru[4,4'-(CH_3)_2bpy]_3^{2+}$;

19. *$Ru(phen)_3^{2+}$; 20. *$Ru(bpy)_3^{2+}$; 21. *$Ru(5\text{-}Cl\ phen)_3^{2+}$; 22. *$Ru[4,7\text{-}(Ch_3)$

22. *$Ru[4,7\text{-}(CH_3)_2phen]_3^{2+}$; 23. *$Os(5\text{-}Cl\ phen)_3^{2+}$, C. Creutz, M. Chou, T.L. Netzel, M. Okumura, and N. Sutin, J. Am. Chem. Soc. 102, 1309 (1980); 24. $Ru[4,7\text{-}(CH_3)_2phen]_3^{3+}$, C.-T. Lin, W. Böttcher, G.M. Brown, C. Creutz, and N. Sutin, J. Am. Chem. Soc. 98, 6536 (1976); 25. $Ru(NH_3)_5py^{3+}$.

* indicates that the oxidant is a photo-excited state reactant.

Figure 4

Plot as for Fig. 3, but involving reductants other than aquo complexes. Key to reactions and data sources: data for macrocycle oxidants are given in Table S5 of ref. 28. 1-5 are cited in ref. 16. 1. $Ru(NH_3)_5py^{3+} + Ru(NH_3)_6^{2+}$; 2. $Ru_{aq}^{3+} + Ru(NH_3)_6^{2+}$; 3. $Co(phen)_3^{3+} + Ru(NH_3)_6^{2+}$; 4. $Co(bpy)_3^{3+} + Ru(NH_3)_6^{2+}$; 5. $Co(phen)_3^{3+} + Ru(NH_3)_5py^{2+}$; 6. horse heart ferricytochrome c + $Ru(NH_3)_6^{2+}$, R.X. Ewall, L.E. Bennett, J. Am. Chem. Soc. 96, 940 (1974); 7. $Co(phen)_3^{3+}$ + horse heart ferrocytochrome c, J.V. McArdle, H.B. Gray, C. Creutz and N. Sutin, J. Am. Chem. Soc. 96, 5737 (1974); 8. $Ru(NH_3)_4bpy^{3+} + Ru(NH_3)_5py^{2+}$, ref. 25.

Figure 5

Plot of $(\Delta G^*_{12} - \Delta G^*_{i,12})$ for homogeneous cross reactions involving oxidation of aquo complexes given in Fig. 3, against the thermodynamic driving force function $-[0.5\Delta G^\circ_{12} + (\Delta G^\circ_{12})^2/16\Delta G^*_{i,12}]$. Closed symbols are obtained from homogeneous data; key to points as in Fig. 3. Open symbols are corresponding points obtained from electrochemical kinetic data for oxidation of aquo cations (see text for details).

FIG 1

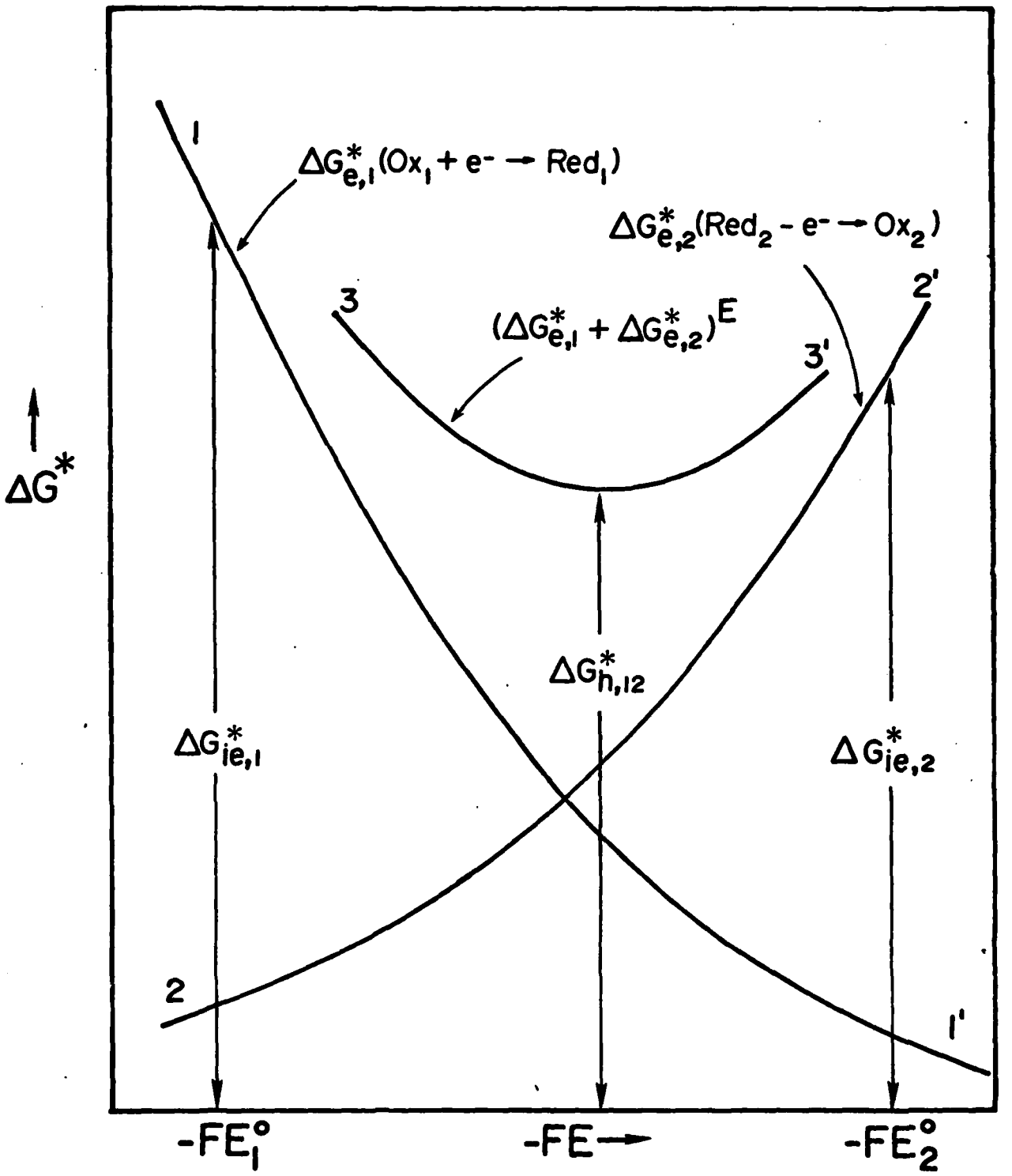
1
$\Delta G^*_{e,1}(Ox_1 + e^- \rightarrow Red_1)$
$\Delta G^*_{e,2}(Red_2 - e^- \rightarrow Ox_2)$
2'
3
$(\Delta G^*_{e,1} + \Delta G^*_{e,2})^E$
3'
ΔG^*
$\Delta G^*_{h,12}$
$\Delta G^*_{ie,1}$
$\Delta G^*_{ie,2}$
2
1'
$-FE^\circ_1$
$-FE \rightarrow$
$-FE^\circ_2$

FIG. 2

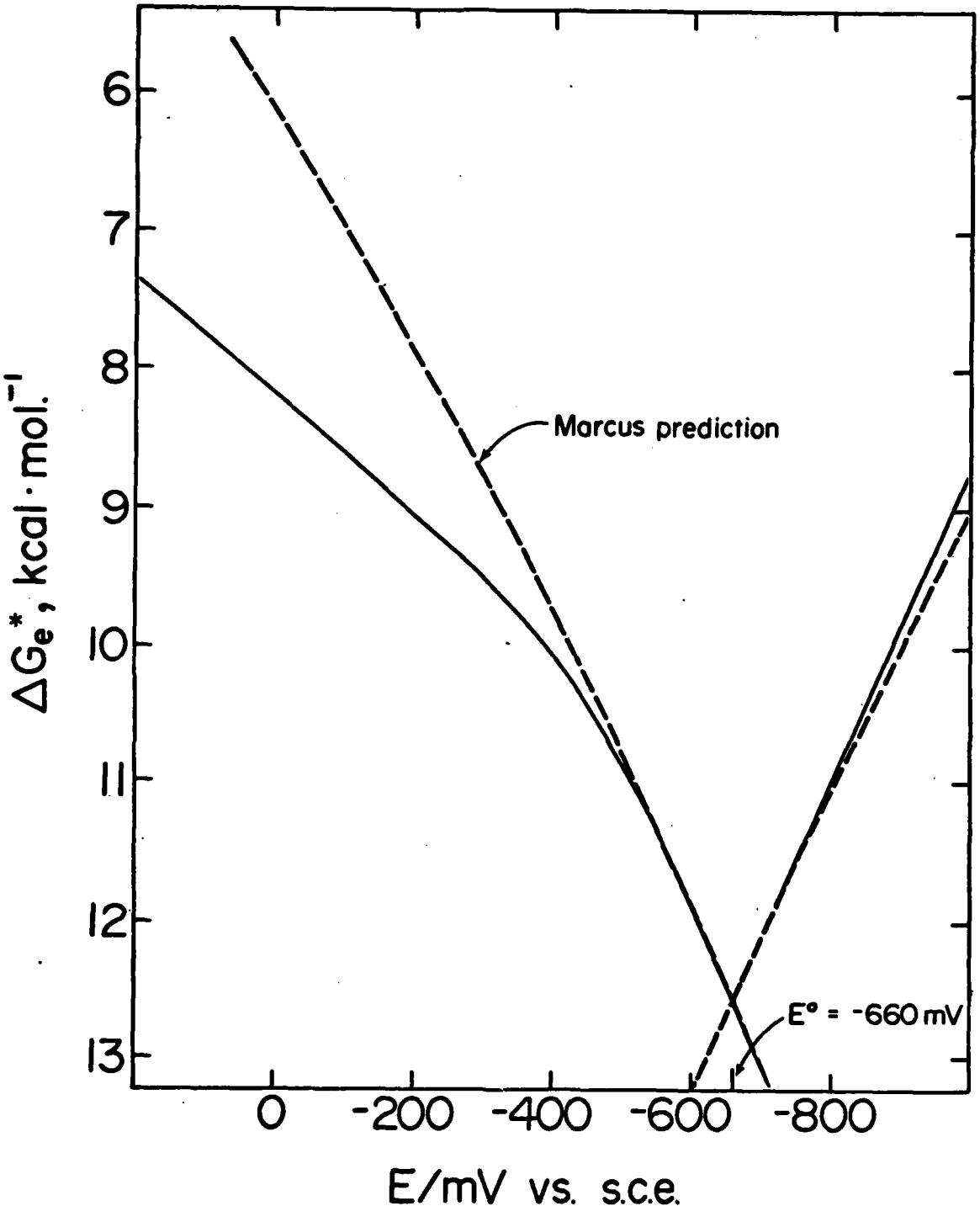
6
7
8
9
10
11
12
13
ΔG_e^*, kcal·mol.$^{-1}$
Marcus prediction
E° = -660 mV
0
-200
-400
-600
-800
E/mV vs. s.c.e.

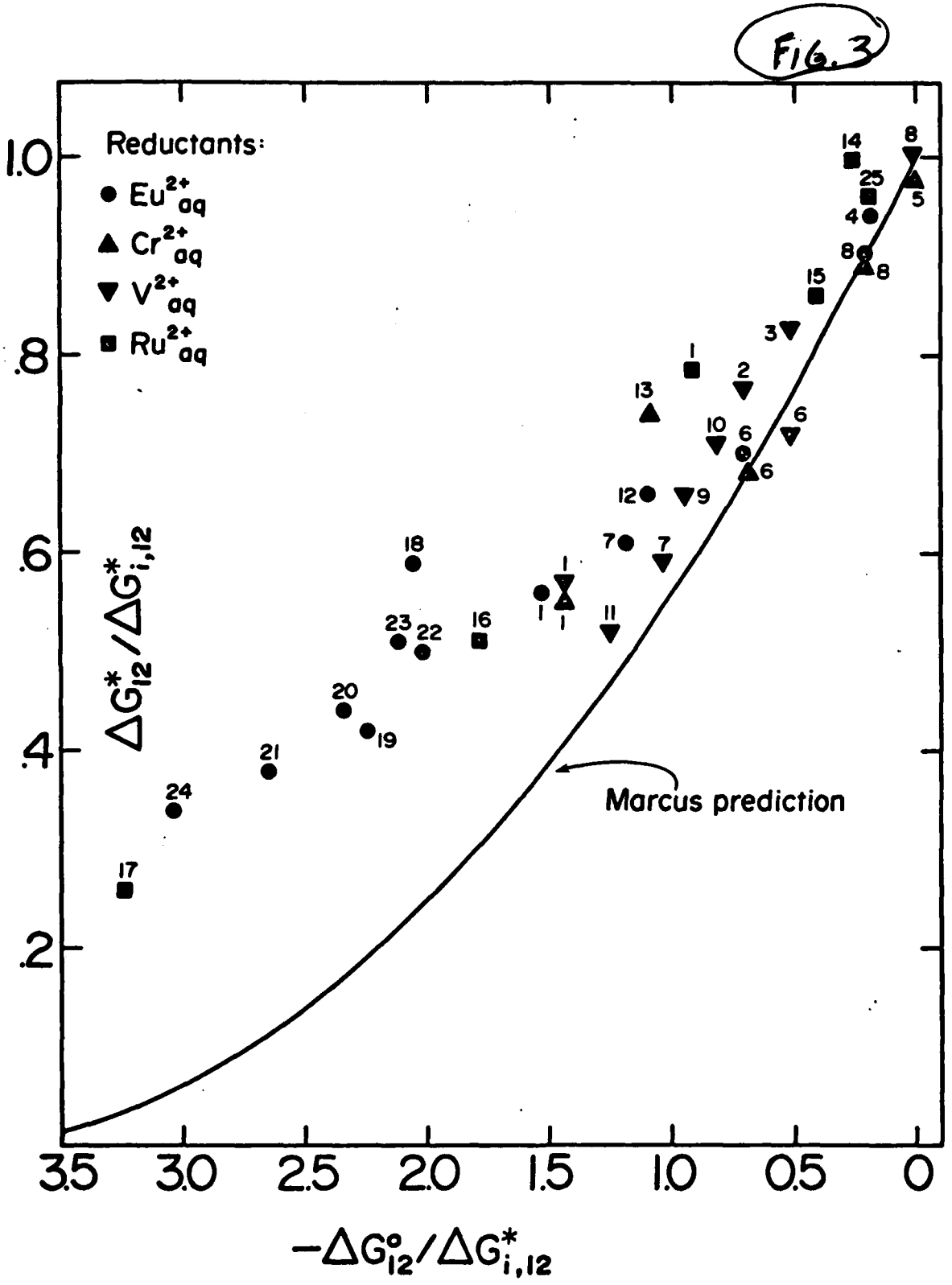
Fig. 3
Reductants:
Eu^{2+}_{aq}
Cr^{2+}_{aq}
V^{2+}_{aq}
Ru^{2+}_{aq}
Marcus prediction
$\Delta G^*_{12}/\Delta G^*_{i,12}$
$-\Delta G^\circ_{12}/\Delta G^*_{i,12}$
1.0
.8
.6
.4
.2
3.5
3.0
2.5
2.0
1.5
1.0
0.5
0

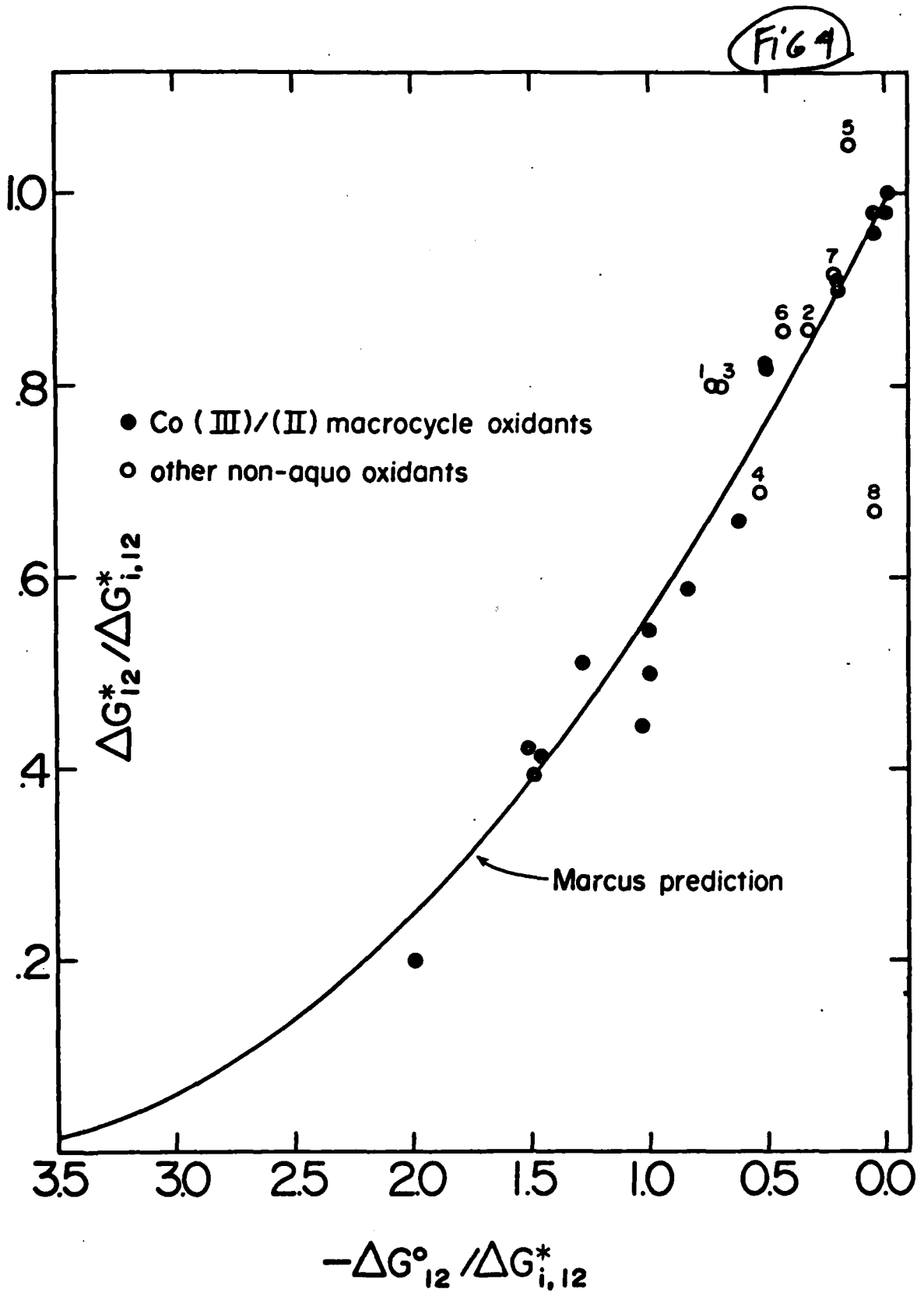
Fig 9
1.0
.8
.6
.4
.2
3.5
3.0
2.5
2.0
1.5
1.0
0.5
0.0
● Co (III)/(II) macrocycle oxidants
o other non-aquo oxidants
Marcus prediction
$\Delta G^*_{12}/\Delta G^*_{i,12}$
$-\Delta G^\circ_{12}/\Delta G^*_{i,12}$

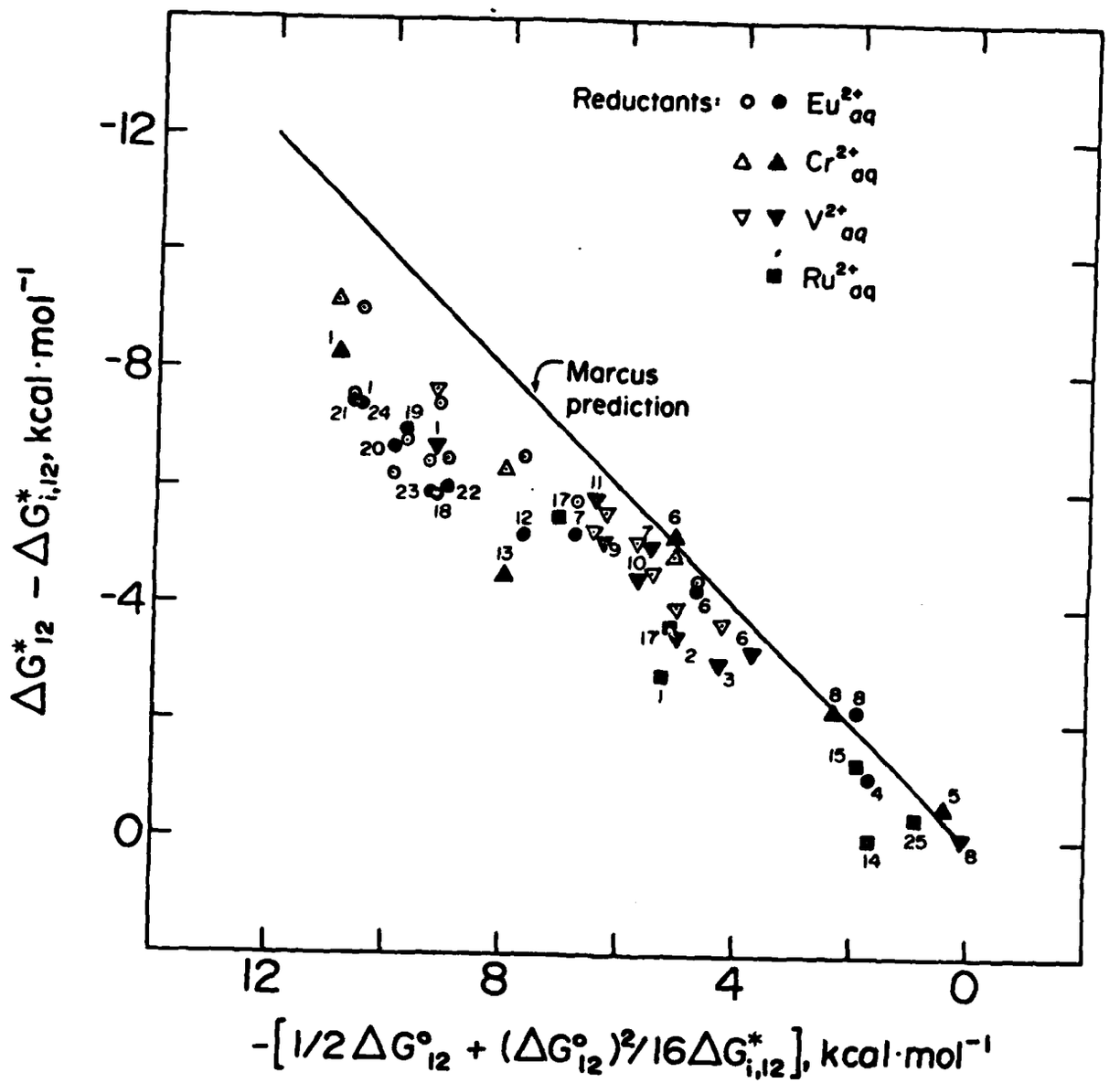
Reductants: Eu2+aq Cr2+aq V2+aq Ru2+aq
Marcus prediction
-12
-8
-4
0
12
8
4
0
ΔG*12 − ΔG*i,12, kcal·mol−1
−[1/2 ΔG°12 + (ΔG°12)2/16ΔG*i,12], kcal·mol−1

FIG. 5

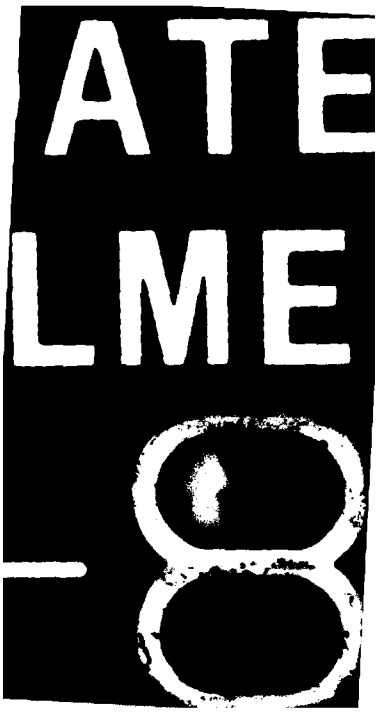
ATE
LME
8